Original Research Article

Potential physiological roles of the 31/32-nucleotide Y4-RNA fragment in human plasma

Sho Ninomiya[1,2], Tatsuya Ishikawa[1], Masayuki Takahashi, Mineaki Seki, Masayuki Nashimoto*

Research Institute for Healthy Living, Niigata University of Pharmacy and Applied Life Sciences, Niigata, Niigata, 956-8603, Japan

ABSTRACT

The 31- and 32-nt 5′-fragments of Y4-RNA (Y4RNAfr) exist abundantly in human plasma. The Y4RNAfr can function as 5′-half-tRNA-type sgRNA for tRNase Z^L, although we do not know yet what its physiological roles are and what cellular RNAs are its genuine targets. In this paper, we analyzed the effects of the Y4RNAfr on cell viability and transcriptomes using HL60, RPMI-8226, and HEK293 cells, and Y4RNAfr-binding RNAs in A549 cells. Although the Y4RNAfr hardly affected the viability of HL60, RPMI-8226, and HEK293 cells, it significantly affected their transcriptome. The DAVID analysis for > 2-fold upregulated and downregulated genes suggested that the Y4RNAfr may affect various KEGG pathways. We obtained 108 Y4RNAfr-binding RNAs in A549 cells, searched potential secondary structures of complexes between theY4RNAfr and its binding RNAs for the pre-tRNA-like structure, and found many such structures. One of the five best fitted structures was for the MKI67 mRNA, suggesting that the Y4RNAfr can decrease the cellular MKI67 level through guiding the cleavage of the MKI67 mRNA by tRNase Z^L. This may be one of the underlying mechanisms for the reported observation that the Y4RNAfr suppresses the proliferation of A549 cells.

1. Introduction

Human Y4-RNA is an ~95-nt non-coding RNA, the gene of which is located on chromosome 7 [1], and appears to be involved in the initiation of DNA replication and RNA quality control [2,3]. We have found that the 31-nt 5′-fragment of Y4-RNA exists abundantly in plasma [4], and have also shown that its 31- and 32-nt 5′-fragments exist in saliva samples after cell removal [5] (Fig. 1A). Repetto et al. [6] have demonstrated that the ~31-nt Y4-RNA fragment exists in sera of coronary artery disease patients more abundantly than in those of controls. Furthermore, Kaudewitz et al. [7] have shown that the ~31-nt Y4-RNA fragment level in plasma correlates with platelet function in patients with acute coronary syndrome and platelet activation markers in a general population. These observations suggest that the ~31-nt Y4-RNA fragment may become a diagnostic/prognostic plasma marker for acute coronary syndrome. In this paper, we collectively call the 3′-heterogenious 31- and 32-nt Y4-RNA fragments Y4RNAfr.

We have discovered Y4RNAfr by analyzing small plasma RNAs from healthy persons and multiple myeloma patients in the course of investigation for the possibility that the intracellular gene regulatory network via tRNase Z^L and small guide RNA (sgRNA) is extended

intercellularly [4,8]. sgRNA is defined as ~7–30-nt RNA that can guide tRNase Z^L to recognize and cleave target RNA by forming a pre-tRNA-like or micro-pre-tRNA-like complex between the target RNA and the sgRNA [9]. miRNAs and degraded RNAs such as 5′-half-tRNAs and rRNA fragments can function as sgRNA [8,10]. It has been shown that the PPM1F and DYNC1H1 mRNAs can be cleaved and downregulated by tRNase Z^L together with the cellular 5′-half-tRNA^{Glu} and the 28S rRNA 3′-terminal fragment, respectively. An sgRNA-mediated gene silencing technology termed tRNase Z^L-utilizing efficacious gene silencing (TRUE gene silencing) is based on this gene regulatory network [11–17].

We have demonstrated that Y4RNAfr can also function as 5′-half-tRNA-type sgRNA for tRNase Z^L, although we do not know yet what its physiological roles are and what cellular RNAs are its genuine targets [4] (Fig. 1B). In any case, the existence in human plasma of Y4RNAfr and the various other potential sgRNAs suggests that the gene regulatory network via tRNase Z^L and sgRNA may be constructed intercellularly as well as intracellularly. In this paper, we investigated what the physiological roles of plasma Y4RNAfr are by analyzing its effects on cell viability and transcriptomes and its binding cellular RNAs using various human cell lines.
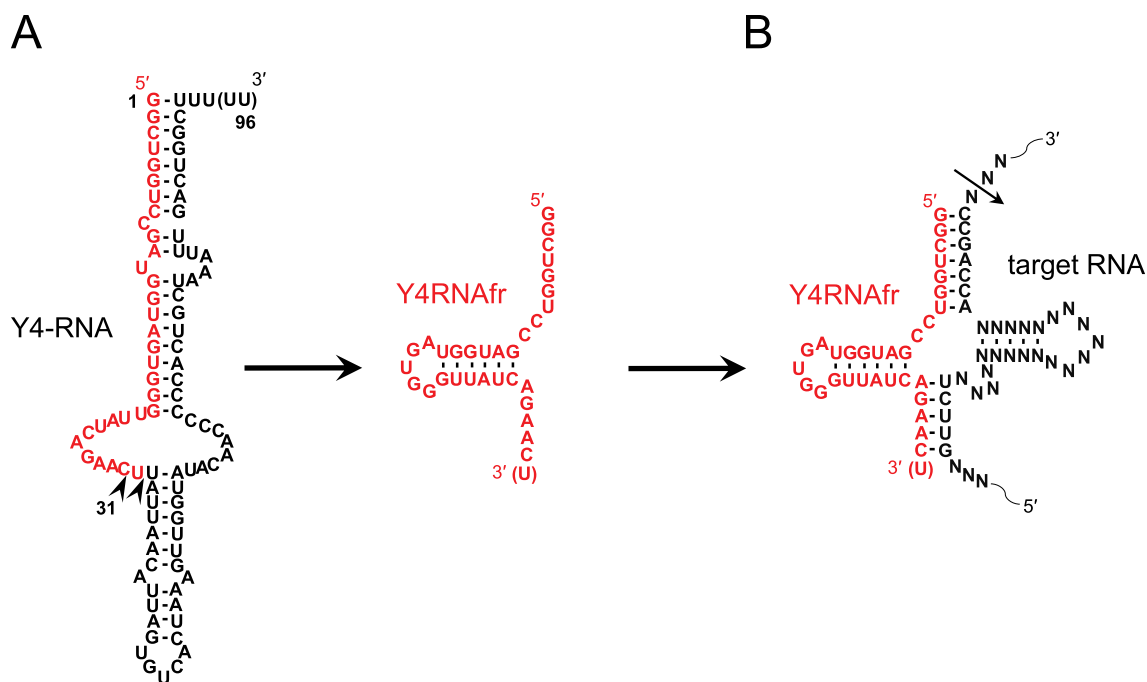
Fig. 1. Human Y4-RNA and its fragments. (A) Human 94–96-nt full-length Y4-RNA and its 31/32-nt 5′-fragments are shown. Arrowheads on the full-length Y4-RNA indicate the cleavage sites to generate the 31- and 32-nt fragments collectively termed Y4RNAfr. (B) A secondary structure of the complex between the Y4RNAfr and a model target RNA. The expected cleavage site by tRNase Z^L is denoted by an arrow.

2. Materials and methods

2.1. RNA preparation

The 31-nt Y4RNAfr (5′-pGGCUGGUCCGAUGGUAGUGGGUUAUCA GAAC-3′) and the five control RNAs CR1 (5′-pUUUUUCUp-3′), CR2 (5′-pGGCCAGGp-3′), CR3 (5′-pCACCAAUp-3′), CR4 (5′-pCACCAAUAGGA UCCp-3′), and CR5 (5′-pCCUGGCCp-3′), which were fully 2′-*O*-methy-lated and 5′/3′-phosphorylated, were synthesized with a DNA/RNA synthesizer and subsequently purified through high-performance liquid chromatography by Nippon Bioservice (Asaka, Saitama, Japan). CR1–CR5 were chosen randomly from our sgRNA library. Likewise, the 31-nt Y4RNAfr (5′-pGGCUGGUCCGAUGGUAGUGGGUUAUCAGAAC-biotin-3′) and the control RNA CR6 (5′-pUCCCUGGUGGUCUAGUGGU UAGGAUUCGGCGCUCU-biotin-3′), which were 5′-phosphorylated and 3′-biotinylated, were synthesized.

2.2. Cell culture

HL60 and RPMI-8226 cells were cultured in RPMI-1640 (Wako, Osaka, Japan) supplemented with 10% fetal bovine serum (MP Biomedicals Japan, Tokyo, Japan) and 1% penicillin-streptomycin (Invitrogen Japan, Tokyo, Japan) at 37 °C in 5% CO_2 humidified in-cubator. HEK293 and A549 cells were cultured in DME media (Wako, Osaka, Japan) likewise. HL60, RPMI-8226, HEK293, and A549 cells were from human promyelocytic leukemia, human myeloma, human embryonic kidney, and human non-small cell lung cancer, respectively.

2.3. Cell viability assay

The human cells were plated at 500 or 1000 cells/100 μl/well on a 96-well dish in media containing 1 μM of the naked Y4RNAfr or CR1. After 3 days, the cell viability was quantitated with Cell Counting Kit-8 (DOJINDO, Tokyo, Japan).

2.4. Transcriptome analysis

HL60 and RPMI-8226 cells (at 80,000 cells/500 μl/well on a 24-well dish) and HEK293 cells (at 20,000 cells/500 μl/well on a 24-well dish) were cultured in media without and with 1 μM of the naked Y4RNAfr. As controls, the cells were also cultured in the presence of 1 μM of naked CR2 or CR3 for HL60 cells, 1 μM of naked CR4 for RPMI-8226 cells, and 1 μM of naked CR5 for HEK293 cells. After one day, each total RNA was extracted with RNAiso Plus (Takara Bio, Shiga, Japan). The RNA samples were subjected to DNA microarray analysis with a SurePrint G3 Human GE v2 8 × 60K Microarray (Agilent Technologies, Tokyo, Japan). This microarray analysis was carried out by Takara Bio (Shiga, Japan).

2.5. RNA pull-down

One day after A549 cells were plated at 150,000 cells/2 ml/well on a 6-well dish, the cells were transfected with 200 pmol of the biotiny-lated Y4RNAfr or CR6 using Lipofectamine 2000 (Thermo Fisher Scientific, Massachusetts, USA) according to manufacturer's protocol. After 18-h incubation, the cells on 6 wells for each RNA treatment were removed with trypsin/EDTA, collected, and washed with phosphate-buffered saline (PBS).

The collected cells were incubated in the presence of 1% for-maldehyde at 37 °C for 10 min, and then further incubated in the presence of 0.5 M glycine at 37 °C for 5 min. After washing the for-maldehyde-treated cells with PBS three times, the cells were suspended in the cell lysis buffer (10 mM HEPES pH7.5, 20 mM KCl, 1.5 mM $MgCl_2$, 0.5 mM EDTA, 1 mM DTT), incubated on ice for 10 min, and homogenized with a Dounce tissue grinder. The homogenate was cen-trifuged at $3300 \times g$ for 7 min, and the supernatant was regarded as a cytoplasmic fraction. The pellet was re-suspended in the nucleus lysis buffer (20 mM HEPES pH7.5, 50 mM KCl, 1.5 mM $MnCl_2$, 1% NP-40, 0.4% sodium deoxycholate, 0.1% N-lauroylsarcosine, 1 mM DTT), so-nicated on ice for 7 min, and centrifuged at $16,000 \times g$ for 10 min. The supernatant was regarded as a nuclear fraction.

The biotinylated Y4RNAfr or CR6 together with its bound nuclear or

cytoplasmic RNAs was purified and collected with Dynabeads M − 270 Streptavidin beads (Thermo Fisher Scientific, Massachusetts, USA) according to manufacturer's protocol. The purified RNA samples were extracted with phenol/chloroform, precipitated with ethanol, and re-dissolved in RNase-free water.

The obtained RNA samples were fragmented to ~60–200-nt RNA with Fragmentation Reagents (Thermo Fisher Scientific, Massachusetts, USA) according to manufacturer's protocol, precipitated with ethanol, and re-dissolved in RNase-free water. The fragmented RNA samples were treated with alkaline phosphatase (Takara Bio, Shiga, Japan) at 50 °C for 30 min, extracted with phenol/chloroform twice, precipitated with ethanol, and re-dissolved in RNase-free water. The dephosphorylated RNA samples were treated with T4 polynucleotide kinase (Takara Bio, Shiga, Japan) and ATP at 37 °C for 30 min, extracted with phenol/chloroform, precipitated with ethanol, and re-dissolved in RNase-free water.

2.6. Next-generation sequencing

A cDNA library was constructed from each of the four RNA samples (~2 μg) using a TruSeq Small RNA Sample Prep Kit (Illumina, California, USA), T4 RNA Ligase 2, truncated (New England Biolabs, Massachusetts, USA), and SuperScript II Reverse Transcriptase (Invitrogen, Massachusetts, USA) by 15 cycles of PCR according to manufacturers' protocols. The cDNAs from the Y4RNAfr-bound nuclear RNA, the CR6-bound nuclear RNA, the Y4RNAfr-bound cytoplasmic RNA, and the CR6-bound cytoplasmic RNA were indexed with the sequences 5′-ATCACG-3′, 5′-TTAGGC-3′, 5′-ACAGTG-3′, and 5′-CAGATC-3′, respectively. A mixture of the four cDNA libraries was separated by polyacrylamide gel electrophoresis, and ~150–300-base-pair cDNAs, which correspond to ~40–190-nt original RNAs, were recovered and purified. The purified cDNA sample was subjected to the next-generation sequencer MiSeq (Illumina). This sequence analysis was carried out by Takara Bio (Shiga, Japan).

2.7. Bioinformatic analysis

Raw signal data obtained from the analysis with the SurePrint G3 Human GE v2 8 × 60K Microarray were imported to a data analytics platform, Subio Platform version 1.22. The microarray contains multiple probes for one gene in a subset of the genes. The raw data of each cell group were normalized globally to adjust means of the raw signal values, and probes that contained at least one abnormal peak signal (gIsFeatNonUnifOL = 1) were removed to obtain filtered data sets. And probes whose signals were < 50 in all samples were also excluded to obtain further filtered data sets. Then we transformed the raw signal values to log2 ratio values by setting the raw signal values in the transcriptome of each Y4RNAfr-treated sample to zero. We extracted genes whose log2 ratio values were < −1.0 and > 1.0 in common in comparison to the transcriptomes of the cell samples that were untreated or treated with the control RNAs.

The RNA sequences obtained by MiSeq were mapped on the human reference genome hg19 in Ensembl (http://asia.ensembl.org/Homo_sapiens/Info/Index), the human reference genome hg38 in National Center for Biotechnology Information (https://www.ncbi.nlm.nih.gov/grc/human), and the human reference genome hg38 in University of California, Santa Cruz (http://genome.ucsc.edu) by Subio (Kagoshima, Japan). The mapped data were analyzed on Subio Platform version 1.22. The Y4RNAfr-pulled-down cellular RNAs, of which raw signal values are more than 10 and more than 5 fold compared with those of RNAs that bound to the control RNA CR6 in at least one of the three mapped data sets, were regarded as Y4RNAfr-bound RNAs.

The genes selected in the DNA microarray analysis and the MiSeq analysis were located on chromosomes using Subio Platform. Data sets of differentially expressed genes and differentially Y4RNAfr-bound RNA genes were further analyzed with a functional annotation tool on the Database for Annotation, Visualization and Integrated Discovery (DAVID) v6.8 (https://david.ncifcrf.gov/summary.jsp) to obtain KEGG pathways implicated in the differences [18–20].

2.8. Search for pre-tRNA-like secondary structures

Each sequence of the genes encoding the Y4RNAfr-bound RNAs was obtained from the database of National Center for Biotechnology Information (https://www.ncbi.nlm.nih.gov). Sequences in each gene complementary to the 5′-terminal sequence 5′-GGCUGGU-3′ and the 3′-terminal sequence 5′-AGAAC-3′ of the Y4RNAfr were searched for using Microsoft Word 2016. One or two mismatches and G-U pairs were allowed. Secondary structures between the Y4RNAfr and each gene RNA sequence were constructed manually to find pre-tRNA-like secondary structures.

2.9. Accession number

DNA microarray data and RNA sequence data were deposited in the DNA Data Bank of Japan (www.ddbj.nig.ac.jp) with the accession numbers E-GEAD-332 and DRR198079–DRR198082, respectively.

3. Results

3.1. The Y4RNAfr hardly affects cell viability

First, we investigated how the Y4RNAfr affects viability of human cultured cells. We cultured HL60 leukemia cells, RPMI-8226 multiple myeloma cells, and HEK293 cells in the presence of the chemically synthesized Y4RNAfr without any transfection reagent for 3 days, and measured their viability. Since the Y4RNAfr was supposed to be added nakedly to the culture media, it was fully 2′-O-methylated and 5′/3′-phosphorylated to protect it from nuclease attack [14]. Under two different cell density conditions, the Y4RNAfr hardly affected the viability of these cells, while the control RNA CR1 tended to decrease their viability (Fig. 2).

3.2. The Y4RNAfr affects transcriptomes

Next, we investigated how the Y4RNAfr affects the transcriptomes of human cells. We cultured HL60, RPMI-8226, and HEK293 cells in the presence of the Y4RNAfr for one day, and performed transcriptome analysis for their total RNA using DNA microarrays. As for the HL60 transcriptome, we extracted genes whose expression level increased and decreased by more than 2 fold in common compared with the expression levels in HL60 cells that were untreated or treated with the control RNA CR2 or CR3, and these genes are listed in Supplementary Table S1. The most increased and decreased 10 genes in comparison with each control transcriptome are also shown in Table 1. Among the top 10 most increased genes, five genes were shared by three comparisons, and two genes were by two comparisons. And among the top 10 most decreased genes, one gene was shared by three comparisons, and four genes were by two comparisons.

Likewise, genes with more than 2-fold increased and decreased expressions were extracted with respect to RPMI-8226 and HEK293 cells (Supplementary Table S1), and the top 10 most increased and decreased genes in comparison with each control transcriptome are listed in Table 1. As for the RPMI-8226 transcriptomes, eight genes among the top 10 most increased genes were common to two comparisons, and no gene was common among the top 10 most decreased genes. As for the HEK293 transcriptomes, five genes among the top 10 most increased genes were common to two comparisons, and three genes among the top 10 most decreased genes were common.

Further analysis of the transcriptome data found that no gene was commonly upregulated or downregulated among HL60, RPMI-8226, and HEK293 cells but that there were some genes commonly
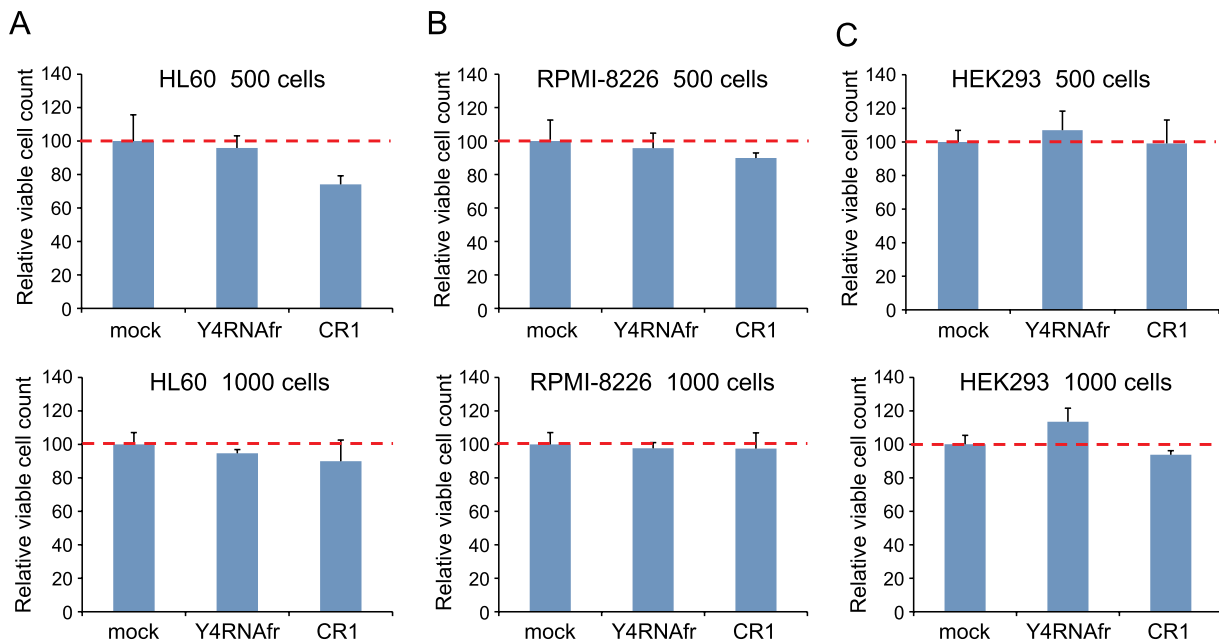
Fig. 2. Cell viability assays. Relative viable cell counts were measured 72 h after HL60 (A), RPMI-8226 (B), or HEK293 (C) cells were cultured in the absence and the presence of 1 μM of the naked Y4RNAfr or CR1. The relative viable cell counts in the absence of the RNAs (mock) are adjusted to 100. Error bars denote standard deviations (n = 3).

upregulated between two cell types. One, six, and three genes were commonly upregulated between HL60 and RPMI-8226 cells, between HL60 and HEK293 cells, and between RPMI-8226 and HEK293 cells, respectively (Table 2). And there was no gene commonly down-regulated between any two cell types.

To see if the genes upregulated and downregulated by the Y4RNAfr treatment are spatially connected, we located the genes extracted for each cell type on the chromosomes (Supplementary Fig. S1). In each case, overall, the genes appear to be located dispersedly, and their notable localization was not detected. However, interestingly, three genes, LRRTM3, DKFZp667F0711, and lnc-NMT2-1, out of the six genes commonly upregulated between HL60 and HEK293 cells were located on chromosome 10 (Supplementary Figs. S1A and C).

Table 2
Commonly upregulated genes between two cell types.

HL60/RPMI-8226	HL60/HEK293	RPMI-8226/HEK293
EXOC6B	LRRTM3	OR5K2
	DKFZp667F0711	ANKRD62
	Q7Z2X8	lnc-ODZ4-2
	CD200R1	
	PLA2G4E	
	lnc-NMT2-1	

Furthermore, we performed the DAVID analysis for the extracted genes of each cell's transcriptome, and found various KEGG pathways involved in the genes whose expression levels were changed by the

Table 1
The top 10 most increased and most decreased genes.

		HL60			RPMI-8226		HEK293	
		CR2	CR3	mock	CR4	mock	CR5	mock
increased	1	lnc-ARFGEF2-3	lnc-ARFGEF2-3	lnc-ARFGEF2-3	KCNJ8	KCNJ8	LOC102723646	LOC102723646
	2	DKFZp667F0711	SPAG17	DKFZp667F0711	PABPC1P2	DISP1	LINC00948	LINC00948
	3	LINC00472	lnc-FZD1-1	LINC00472	XLOC_l2_000080	ENPP1	MAMDC2	lnc-DPYD-2
	4	OR2T2	DKFZp667F0711	OR2T2	ENPP1	XLOC_l2_000080	lnc-ZNF280D-1	LRRTM3
	5	LOC100129781	SPATA31D3	ABCC13	lnc-C8orf59-1	LOC101928796	LOC100996844	lnc-ZNF280D-1
	6	ABCC13	LOC102723456	ZNF793	LOC101928796	LRTM2	SNORD115-5	lnc-C17orf97-7
	7	SKOR2	LINC00472	PRR27	LRTM2	lnc-FAM49A-1	lnc-IGF1R-1	SNORD115-5
	8	ZNF793	OR2T2	LINC01085	DISP1	lnc-COPS4-1	CTNNA3	LOC100996844
	9	lnc-PIGP-1	lnc-SLC4A3-8	lnc-C10orf90-2	lnc-COPS4-1	SPINK2	lnc-C3orf38-2	lnc-TPBG-3
	10	lnc-FZD1-1	ABCC13	CCK	SPINK2	LOC101929911	MYADML	LOC340340
decreased	1	SPATA3-AS1	lnc-C5orf64-1	SPATA3-AS1	MAP7D2	ADAMTS4	MCHR2	LOC102467226
	2	KRTAP5-4	lnc-FAM110B-1	C7orf76	LRRC63	lnc-C15orf2-6	F13A1	SYNPR
	3	UNC80	OR2T34	GRAP	lnc-USPL1-2	lnc-TCF4-4	OR2F1	LOC101060038
	4	lnc-CCDC37-3	ZNF528	LOC101927204	lnc-CD99L2-2	lnc-PFDN1-1	LOC102467226	LOC101927291
	5	SIGLEC9	lnc-RP3-368B9.1.1–4	lnc-PDGFD-5	LINC01013	ZNF365	LOC102723597	LOC440446
	6	lnc-PDGFD-5	lnc-PDGFD-5	lnc-SERPINI1-9	GALNT13	lnc-BATF3-2	APELA	GSTA3
	7	lnc-CMPK2-1	lnc-CMPK2-1	TTN	LOC102723778	OR9Q2	NCRNA00250	lnc-CMPK2-13
	8	lnc-METTL15-4	XLOC_l2_004640	XLOC_l2_010969	lnc-FAM135B-2	SVILP1	ITGAL	NCRNA00250
	9	LOC101927204	lnc-SERPINI1-9	LINC00935	IFNA7	HRASLS	ACTA2-AS1	ACTA2-AS1
	10	LOC101928725	lnc-CLASP2-1	LOC101927136	SLCO2A1	DEFB109P1	LOC101929756	LOC100131023

Table 3
KEGG pathways involved in genes whose expression levels were changed by Y4RNAfr.

Cell	Term	Count	%	P-Value
HL60	Tight junction	4	3.1	5.10E-03
	Olfactory transduction	5	3.8	7.60E-02
	Histidine metabolism	2	1.5	8.60E-02
RPMI-8226	Antigen processing and presentation	7	1.8	5.00E-04
	Type I diabetes mellitus	5	1.3	2.30E-03
	Autoimmune thyroid disease	5	1.3	5.00E-03
	Staphylococcus aureus infection	5	1.3	5.70E-03
	Asthma	4	1	7.20E-03
	Graft-versus-host disease	4	1	9.50E-03
	Allograft rejection	4	1	1.30E-02
	Toxoplasmosis	6	1.5	1.60E-02
	Intestinal immune network for IgA production	4	1	2.50E-02
	Tuberculosis	7	1.8	3.10E-02
	Neuroactive ligand-receptor interaction	9	2.3	3.10E-02
	Viral myocarditis	4	1	4.00E-02
	PI3K-Akt signaling pathway	10	2.6	4.00E-02
	Phagosome	6	1.5	5.00E-02
	Inflammatory bowel disease (IBD)	4	1	5.40E-02
	Regulation of actin cytoskeleton	7	1.8	6.20E-02
	Leishmaniasis	4	1	6.90E-02
	Pathways in cancer	10	2.6	7.90E-02
	Influenza A	6	1.5	8.30E-02
	Olfactory transduction	10	2.6	8.50E-02
HEK293	Complement and coagulation cascades	4	2.5	4.60E-03
	Staphylococcus aureus infection	3	1.9	2.90E-02
	Arachidonic acid metabolism	3	1.9	3.60E-02
	Salmonella infection	3	1.9	6.30E-02
	Rheumatoid arthritis	3	1.9	7.00E-02
	Toll-like receptor signaling pathway	3	1.9	9.60E-02

Y4RNAfr (Table 3). The Y4RNAfr appears to affect the olfactory transduction pathway commonly in HL60 and RPMI-8226 cells and the *Staphylococcus aureus* infection pathway commonly in RPMI-8226 and HEK293 cells (Table 3).

Table 4
KEGG pathways involved in Y4RNAfr-bound RNA genes.

Term	Count	%	P-Value
Ascorbate and aldarate metabolism	10	8.3	2.00E-13
Pentose and glucuronate interconversions	9	7.4	8.60E-11
Porphyrin and chlorophyll metabolism	9	7.4	6.90E-10
Retinol metabolism	10	8.3	9.40E-10
Drug metabolism - other enzymes	9	7.4	1.50E-09
Steroid hormone biosynthesis	9	7.4	1.00E-08
Drug metabolism - cytochrome P450	9	7.4	3.70E-08
Metabolism of xenobiotics by cytochrome P450	9	7.4	7.30E-08
Chemical carcinogenesis	9	7.4	1.40E-07
Metabolic pathways	15	12.4	7.40E-02

3.3. Cellular RNAs that bind to the Y4RNAfr

Next, we investigated what RNAs the Y4RNAfr binds to in cells. We transfected human A549 cells with the 3′-biotinylated Y4RNAfr, and sequenced nuclear and cytoplasmic RNAs that bound to the Y4RNAfr. The RNAs, of which raw signal values are more than 10 and more than 5 fold compared with those of RNAs that bound to the control RNA CR6, were regarded as Y4RNAfr-bound RNAs, and further analyzed. 40 and 68 RNA species were selected as nuclear and cytoplasmic RNAs, respectively, that bind to the Y4RNAfr (Supplementary Table S2). Then we located the genes encoding these RNAs on the chromosomes, and found that, on the whole, these genes are located dispersedly without any notable localization (Supplementary Fig. S2).

We searched potential secondary structures of cellular RNA/Y4RNAfr complexes for the pre-tRNA-like structure, and found many such structures. The five best fitted structures were obtained for COL7A1, IQGAP1, MKI67, CHD3, and EHBP1 mRNAs (Fig. 3).

We also carried out the DAVID analysis for the genes of the 108 Y4RNAfr-bound RNAs, and found 10 KEGG pathways including ascorbate and aldarate metabolism, pentose and glucuronate interconversions, and porphyrin and chlorophyll metabolism, which may be affected by the Y4RNAfr (Table 4). Lastly, it should be noted that the gene encoding one of the cytoplasmic Y4RNAfr-bound RNAs is ELAC2 that encodes tRNase Z^L (Supplementary Table S2).
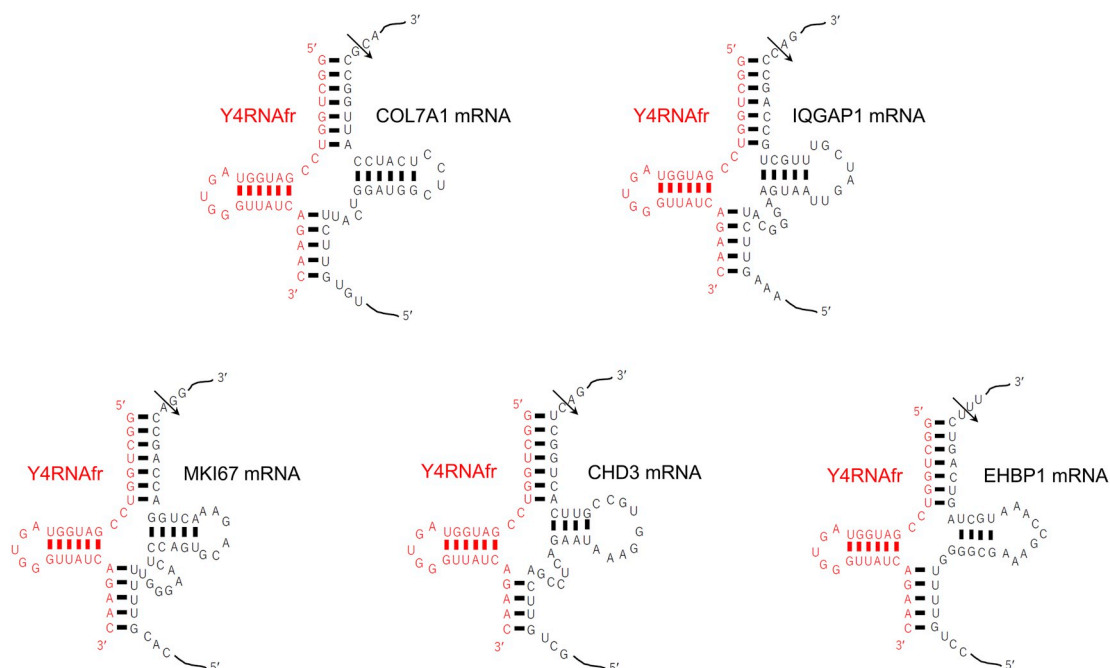

Fig. 3. Potential secondary structures of the complexes between the 31-nt Y4RNAfr and the COL7A1, IQGAP1, MKI67, CHD3, or EHBP1 mRNA. The arrow indicates the expected cleavage site by tRNase Z^L.

4. Discussion

In this paper, to investigate what the physiological roles of the plasma Y4RNAfr are, we analyzed the effects of the Y4RNAfr on cell viability and transcriptomes using HL60, RPMI-8226, and HEK293 cells, and Y4RNAfr-binding RNAs in A549 cells. Although the Y4RNAfr hardly affected the viability of HL60, RPMI-8226, and HEK293 cells, it significantly affected their transcriptome. As for the Y4RNAfr-treated HL60 cells, 163 and 33 genes were upregulated and downregulated, respectively, by more than 2 fold in common compared with the untreated cells and the CR2-and CR3-treated cells (Supplementary Table S1). And the DAVID analysis for these genes suggested that the Y4RNAfr may be involved in tight junctions, olfactory transduction, and histidine metabolism (Table 3).

As for the Y4RNAfr-treated RPMI-8226 cells, 509 and 74 genes were upregulated and downregulated, respectively, in common compared with the untreated cells and the CR4-treated cells (Supplementary Table S1). Twenty KEGG pathways including antigen processing and presentation, type I diabetes mellitus, and autoimmune thyroid disease were suggested to be affected by the Y4RNAfr (Table 3).

With respect to HEK293 cells, 211 and 24 genes were upregulated and downregulated, respectively, by the Y4RNAfr in common compared with the untreated cells and the CR5-treated cells (Supplementary Table S1). Six KEGG pathways including complement and coagulation cascades, *Staphylococcus aureus* infection, and arachidonic acid metabolism appeared to be affected by the Y4RNAfr treatment (Table 3).

With respect to human monocytes/macrophages, it has been shown that the Y4RNAfr regulates cell death and inflammation via TLR7 [21]. In addition, the Y4RNAfr has been demonstrated to modulate cytokine release and PD-L1 expression via TLR7 in monocytes [22].

Concerning human non-small cell lung cancer A549 cells, their proliferation has been shown to be suppressed by the Y4RNAfr [23]. The present analysis suggested that the Y4RNAfr affects the 10 KEGG pathways in A549 cells (Table 4). In addition, among potential secondary structures of cellular RNA/Y4RNAfr complexes, one of the five best structures fitted to the pre-tRNA-like structure was with the MKI67 mRNA (Fig. 3). This suggests that the Y4RNAfr may suppress the proliferation of A549 cells by decreasing the MKI67 level through guiding the cleavage of the MKI67 mRNA by tRNase Z^L, since it is known that MKI67 is associated with ribosomal RNA transcription and that the decrease in the MKI67 level suppresses cell proliferation [24].

Our present observations together with other groups' observations suggest that the Y4RNAfr in plasma has various physiological roles in various types of cells. And finally, the possibilities of modulation of the tRNase Z^L level through Y4RNAfr binding to tRNase Z^L (ELAC2) mRNA and modulation of the MKI67 level through the cleavage of the MKI67 mRNA by tRNase Z^L under the direction of the Y4RNAfr may support the existence of the intercellular gene regulatory network via tRNase Z^L and sgRNA.

Declaration of competing interest

The authors declare no competing interests.

References

[1] R.J. Maraia, N. Sasaki-Tozawa, C.T. Driscoll, et al., The human Y4 small cytoplasmic RNA gene is controlled by upstream elements and resides on chromosome 7 with all other hY scRNA genes, Nucleic Acids Res. 22 (1994) 3045–3052.

[2] A.T. Zhang, A.R. Langley, C.P. Christov, et al., Dynamic interaction of Y RNAs with chromatin and initiation proteins during human DNA replication, J. Cell Sci. 124 (2011) 2058–2069.

[3] S. Sim, S.L. Wolin, Emerging roles for the Ro 60-kDa autoantigen in noncoding RNA metabolism, Wiley Interdiscipl. Rev. RNA 2 (2011) 686–699.

[4] S. Ninomiya, M. Kawano, T. Abe, et al., Potential small guide RNAs for tRNase ZL from human plasma, peripheral blood mononuclear cells, and cultured cell lines, PLoS One 10 (2015) e0118631.

[5] T. Ishikawa, A. Haino, M. Seki, et al., The Y4-RNA fragment, a potential diagnostic marker, exists in saliva, Non Coding RNA Res. 2 (2017) 122–128.

[6] E. Repetto, L. Lichtenstein, Z. Hizir, et al., RNY-derived small RNAs as a signature of coronary artery disease, BMC Med. 13 (2015) 259.

[7] D. Kaudewitz, P. Skroblin, L.H. Bender, et al., Association of microRNAs and YRNAs with platelet function, Circ. Res. 118 (2016) 420–432.

[8] R.A. Elbarbary, H. Takaku, N. Uchiumi, et al., Modulation of gene expression by human cytosolic tRNase Z^L through 5′-half-tRNA, PLoS One 4 (2009) e5908.

[9] H.S. Shibata, H. Takaku, M. Takagi, et al., The T loop structure is dispensable for substrate recognition by tRNase ZL, J. Biol. Chem. 280 (2005) 22326–22334.

[10] R.A. Elbarbary, H. Takaku, N. Uchiumi, et al., Human cytosolic tRNase ZL can downregulate gene expression through miRNA, FEBS Lett. 583 (2009) 3241–3246.

[11] Y. Habu, N. Miyano-Kurosaki, M. Kitano, et al., Inhibition of HIV-1 gene expression by retroviral vector-mediated small-guide RNAs that direct specific RNA cleavage by tRNase ZL, Nucleic Acids Res. 33 (2005) 235–243.

[12] A. Nakashima, H. Takaku, H.S. Shibata, et al., Gene-silencing by the tRNA maturase tRNase Z^L under the direction of small guide RNA, Gene Ther. 14 (2007) 78–85.

[13] R.A. Elbarbary, H. Takaku, M. Tamura, et al., Inhibition of vascular endothelial growth factor expression by TRUE gene silencing, Biochem. Biophys. Res. Commun. 379 (2009) 924–927.

[14] M. Takahashi, R.A. Elbarbary, A. Nakashima, et al., A naked RNA heptamer targeting the human Bcl-2 mRNA induces apoptosis of HL60 leukemia cells, Cancer Lett. 328 (2013) 362–368.

[15] N. Watanabe, M. Narita, A. Yamahira, et al., Induction of apoptosis of leukemic cells by TRUE gene silencing using small guide RNAs targeting the WT1 mRNA, Leuk. Res. 37 (2013) 580–585.

[16] S. Iizuka, N. Oridate, M. Nashimoto, et al., Growth inhibition of head and neck squamous cell carcinoma cells by sgRNA targeting the cyclin D1 mRNA based on TRUE gene silencing, PLoS One 9 (2014) e114121.

[17] A. Haino, T. Ishikawa, M. Seki, et al., TRUE gene silencing: screening of a heptamer-type small guide RNA library for potential cancer therapeutic agents, J. Vis. Exp. (2016), https://doi.org/10.3791/53879.

[18] D.W. Huang, B.T. Sherman, R.A. Lempicki, Systematic and integrative analysis of large gene lists using DAVID bioinformatics resources, Nat. Protoc. 4 (2009) 44–57.

[19] D.W. Huang, B.T. Sherman, R.A. Lempicki, Bioinformatics enrichment tools: paths toward the comprehensive functional analysis of large gene lists, Nucleic Acids Res. 37 (2009) 1–13.

[20] H. Ogata, S. Goto, K. Sato, et al., KEGG: kyoto encyclopedia of genes and genomes, Nucleic Acids Res. 27 (1999) 29–34.

[21] Z. Hizir, S. Bottini, V. Grandjean, et al., RNY (YRNA)-derived small RNAs regulate cell death and inflammation in monocytes/macrophages, Cell Death Dis. 8 (2017) e2530.

[22] F. Haderk, R. Schulz, M. Iskar, et al., Tumor-derived exosomes modulate PD-L1 expression in monocytes, Sci. Immunol. 2 (2017) pii: eaah5509.

[23] C. Li, F. Qin, F. Hu, et al., Characterization and selective incorporation of small non-coding RNAs in non-small cell lung cancer extracellular vesicles, Cell Biosci. 8 (2018) 2.

[24] J. Bullwinkel, B. Baron-Lühr, A. Lüdemann, et al., Ki-67 protein is associated with ribosomal RNA transcription in quiescent and proliferating cells, J. Cell. Physiol. 206 (2006) 624–635.